Biotic contribution to air-sea fluxes of CO_2 and O_2 and its relation to new production, export production, and net community production

Andreas Oschlies and Paul Kähler
Institut für Meereskunde an der Universität Kiel, Kiel, Germany

Received 19 May 2003; revised 7 November 2003; accepted 1 December 2003; published 28 January 2004.

[1] The contribution of the marine biota to air-sea fluxes of CO_2 and O_2 is often described in terms of biological production concepts, such as new production, export production, and net community production. We evaluate these three quantities using a basin-scale ecosystem-circulation model of the North Atlantic Ocean based on Redfield stoichiometry into which we introduce an artificial tracer which records the biotic contribution to air-sea exchange of gases like O_2 and CO_2. It is found that on average the biological production rates overestimate the biotically effected air-sea flux by some 20% and, in some regions, even predict the wrong direction. With primary production restricted to the euphotic zone, but respiration extending to farther below, the discrepancy can largely be attributed to the different integration depths used in the different concepts (euphotic zone, surface mixed layer), and on annual and longer timescales, all rates converge when using the base of the winter mixed layer rather than that of the euphotic zone as the reference depth. For the surface carbon budget, which ultimately controls air-sea exchange of CO_2, it is irrelevant whether carbon atoms cross this boundary in organic or inorganic speciation. Hence the transports of biotically generated surpluses or deficits of dissolved inorganic matter must also be accounted for. While their contribution amounts to only a few percent on the basin scale, the subduction of newly remineralized inorganic matter can locally account for about half of the biotically effected air-sea flux, for example, in regions of mode-water formation. *INDEX TERMS:* 4805 Oceanography: Biological and Chemical: Biogeochemical cycles (1615); 4806 Oceanography: Biological and Chemical: Carbon cycling; 4845 Oceanography: Biological and Chemical: Nutrients and nutrient cycling; 4842 Oceanography: Biological and Chemical: Modeling; *KEYWORDS:* air-sea gas exchange, biological pump, marine carbon cycle

Citation: Oschlies, A., and P. Kähler (2004), Biotic contribution to air-sea fluxes of CO_2 and O_2 and its relation to new production, export production, and net community production, *Global Biogeochem. Cycles*, *18*, GB1015, doi:10.1029/2003GB002094.

1. Introduction

[2] Photosynthesis reduces the partial pressure of carbon dioxide (pCO_2) in the ocean's surface waters. This allows the ocean to take up more CO_2 from the atmosphere than a hypothetical abiotic ocean would. Respiration of organic matter releases CO_2, thus counteracting this uptake. A net effect on the ocean's carbon inventory, and hence on the partitioning of carbon between atmospheric and oceanic reservoirs, is only achieved because photosynthesis and respiration do not balance locally. As a result of the gravitational settling of particulate organic matter and transports of carbon species by advection and turbulent mixing, respiration on average takes place deeper in the water column than photosynthetic fixation of organic carbon, which is confined to the light-lit surface layer (the euphotic zone, often operationally defined by the 1% light level and typically the upper 100 m of the ocean). The downward transport of organic carbon which effects a net pCO_2 drawdown in the surface waters is commonly termed the "soft tissue" pump [*Volk and Hoffert*, 1985]. A related pump, the "carbonate" pump, is driven by the downward transport of calcium carbonate "hard parts." In terms of CO_2, this is a counter pump, since the formation of calcium carbonate increases pCO_2. The "soft tissue" pump (often in combination with the "carbonate" pump) is commonly referred to as the "biological" carbon pump. It is responsible for about three fourths of the observed vertical gradient of dissolved inorganic carbon (DIC) in the ocean [*Sarmiento and Siegenthaler*, 1992], the remainder being generated abiotically by the "solubility" pump, which is caused by the variation of CO_2 solubility along meridional temperature gradients and the three-dimensional oceanic ventilation pattern.

[3] In steady state, neither of these carbon pumps generates a global net air-sea flux of CO_2 (inherent in steady state). The shortest time to consider steady state is 1 year,

Copyright 2004 by the American Geophysical Union.
0886-6236/04/2003GB002094$12.00

which cancels out seasonally cyclic changes of organic-matter stocks. In steady state, the biotically mediated downward flux of carbon is balanced by an upward return flux at any depth level (not necessarily at the same location). Small amounts of carbon buried in the sediments are ignored in the context of this study, as are terrestrial inputs. *Volk and Hoffert* [1985] defined the strength of the biological pump as the biotically effected DIC concentration difference between surface and deep ocean, i.e., as a measure of potential rather than of rates or processes. Its application to simple box models is straightforward, as in these models the water column is typically partitioned into two boxes only, one representing the surface layer, the other the deep ocean. Conceptual difficulties arise when resolving continuous vertical profiles and lateral and seasonal variation.

[4] Alternative, flux-based concepts of biological processes relevant to the global carbon cycle focus on rates of transformations and transports which maintain the vertical gradients of DIC and nutrients against the leveling action of diffusion and circulation. Among them are new production (NP), export production (EP), and net community production (NCP). Historically, these concepts were introduced as descriptions of the potentially exploitable yield of marine ecosystems (*Dugdale and Goering* [1967] for NP, *Eppley and Peterson* [1979] for EP). More recently, interest in the fate of anthropogenic CO_2 emissions shifted attention to the air-sea exchange of CO_2. In attempts to quantify the biotically effected DIC drawdown, sometimes the biological pump is equated with export production, new production, or net community production [e.g., *Sarmiento and Siegenthaler*, 1992; *Sambrotto et al.*, 1993; *del Giorgio et al.*, 1997; *Prentice et al.*, 2001] often assuming the three of them, implicitly or explicitly, to be the same [*Williams*, 1993]. A careful data-based investigation of the biological pump's impact on air-sea CO_2 exchange was presented by *Koeve* [2002] and addressed the issues of an adequate reference depth as well as effects of the carbonate pump.

[5] In the present study, we compare the biological rates of NP, EP, and NCP with the biotically effected air-sea exchange of gases like CO_2 and O_2 in the context of a model which combines an elaborate high-resolution physical model of the North Atlantic with a simple four-compartment nitrogen-based ecosystem model. On the one hand, its finer spatial and temporal resolution provides a more realistic setting than achievable by box models. On the other hand, the biological model presents a highly simplified picture of the real marine ecosystem. All fluxes are computed in nitrogen units, with a constant Redfield stoichiometry relating nitrogen and carbon. In particular, the model neglects nitrogen fixation, denitrification, the formation of carbon-rich organic matter (e.g., dissolved organic matter, DOM), and calcification. All these processes will, in reality, affect the air-sea exchange of CO_2 and/or O_2. However, present knowledge of their physiological and ecological significance as well as their controlling factors is at best qualitative, which makes them difficult to parameterize quantitatively in any model. We therefore begin our analysis of biotically effected air-sea exchange and biological production concepts by excluding these non-Redfield processes altogether, being aware that future refinements will have to reconsider them. For the time being, their neglect is for the sake of both simplicity and consistency. By confining the effect of organisms to that of organic particles (tissues rather than shells and exudates) of Redfield C:N ratios, an internally consistent model environment is created in which, according to current conceptual understanding, the different biological production concepts should work coherently. In the main part of this study we also neglect physical and chemical controls on the kinetics of air-sea gas exchange and instead assume instantaneous equilibration of sea surface concentrations with the atmosphere. Even in this simple and internally consistent picture, the steady-state biological production rates turn out to be not equivalent, neither among themselves nor with the biotically effected air-sea fluxes of CO_2 and O_2.

[6] The paper is organized as follows: Section 2 will briefly describe the coupled ecosystem-circulation model. Our approach to measure the impact of marine biota on the air-sea exchange of CO_2 and O_2 in a seasonally varying ocean will be described in section 3. Discrepancies among biotically effected air-sea exchange and new production, export production, and net community production are examined in section 4, and a reconciliation of the different concepts is presented in section 5. Section 6 addresses the issue of different air-sea gas exchange velocities and timescales longer than the annual cycle. A concluding discussion highlights some pitfalls in the application of the traditional biological production concepts to the ocean carbon budget.

2. Numerical Model

[7] The present configuration of our numerical ecosystem model is a simple four-component nitrate-phytoplankton-zooplankton-detritus (NPZD) model [*Oschlies and Garçon*, 1999] augmented by a particle aggregation model [*Kriest and Evans*, 1999; *Kriest*, 2002] (Figure 1). The aggregation model solves a conservation equation for the number of particles. From total mass and particle numbers, it diagnoses the exponent of a power-law size-class spectrum for each grid point and each time step, and the resulting aggregate size spectrum allows the computation of effective sinking rates of phytoplankton and detritus. In contrast to previous versions lacking the aggregation model, both phytoplankton and detritus have temporally and spatially varying sinking velocities. The annual mean sinking speed at a depth of 126 m, for example, varies from less than 1 m/day in the subtropics to more than 5 m/day at high latitudes and in the equatorial and coastal upwelling regions. Maximum sinking velocities at the same depth exceed 10 m/day almost everywhere north of 40°N (Figure 2). Annually averaged primary production and nutrient input to surface water are very similar to the results of the previous model version which used a constant sinking velocity (of detritus only) of 5 m/day [*Oschlies et al.*, 2000; *Oschlies*, 2002]. The main impact of the aggregation model is its ability to simulate rapid and deep export of organic matter following the spring bloom at middle and high latitudes. Test runs with the older model version showed this to make little change compared

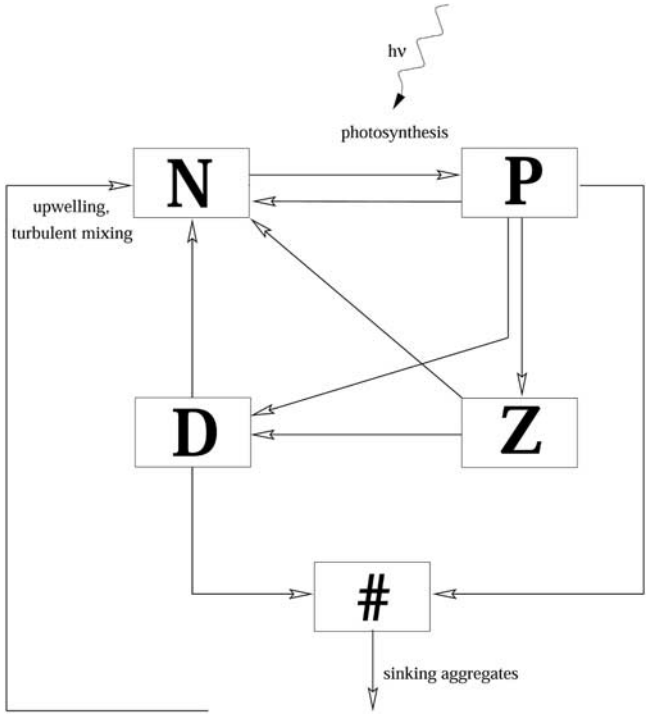

Figure 1. Compartments and interactions of the pelagic ecosystem model. Primary production is represented by the arrow from dissolved inorganic nitrogen (N) to phytoplankton (P), and respiration is represented by the sum of the arrows from phytoplankton (P) to N, from zooplankton (Z) to N, and from detritus (D) to N. See *Oschlies and Garçon* [1999] and *Kriest* [2002] for a detailed description.

to the results presented here. The present model configuration does not include a sediment model, so all organic matter which reaches the bottom remains in the deepest grid box where it is subject to advection, mixing, and remineralization. All standing stocks and all fluxes are computed in nitrogen units. To convert nitrogen into carbon, we employ the standard Redfield ratio (6.625 mol C/mol N) throughout.

[8] The ecosystem model is embedded into an eddy-permitting circulation model of the North Atlantic at $(2/5)^\circ \times (1/3)^\circ$ (zonal $\times$ meridional) resolution based on the Geophysical Fluid Dynamics Laboratory's (GFDL) Modular Ocean Model (MOM [*Pacanowski et al.*, 1991]). It resolves 37 vertical levels with 11 levels in the uppermost 150 m. Vertical mixing is modeled by a turbulent kinetic energy (TKE) closure scheme [*Gaspar et al.*, 1990] tuned to closely match observational estimates of diapycnal diffusion derived from a tracer-release experiment in the main thermocline of the eastern subtropical North Atlantic [*Ledwell et al.*, 1993, 1998]. Atmospheric forcing consists of "climatological" monthly mean wind-stress and heat-flux fields from the years 1989 to 1993 of the reanalysis project carried out at the European Centre for Medium-Range Weather Forecasts (ECMWF) [*Gibson et al.*, 1997]. The formulation of the non-solar part of the surface heat flux follows *Haney* [1971] with a flux-correction term that accounts for a heat-flux feedback from simulated surface temperature anomalies [*Barnier et al.*, 1995]. Freshwater fluxes are parameterized by restoring surface salinity to observed monthly means taken from the *Levitus et al.* [1994] atlas. To account for water mass transformation outside the North Atlantic model domain, temperature, salinity, and nitrate are restored to climatological data in buffer zones (five grid points wide) at the closed northern and southern boundaries.

[9] Simulated biogeochemical properties in the upper ocean were found to reach a relatively stable seasonal cycle already after 2 years [e.g., *Oschlies and Garçon*, 1999, Figure 2]. With the aim to achieve a better adjustment of deeper layers, the coupled ecosystem-circulation model was integrated for 20 years, and model results shown are averaged over the sixteenth to twentieth year of the coupled model. In retrospect we know that results shown below would not differ significantly had we chosen the third to seventh year (as in previous applications of the model). Before coupling with the biological model, the physical model had been spun up in a 25-year integration starting from rest at climatological temperature and salinity fields.

3. Illustration of Concepts

3.1. Yield of the Biological Pump

[10] All air-sea exchange, whether driven physically or biotically, concerns the same molecules, and in reality, there is no direct way to distinguish between the effects of physics and biota. In our model we can isolate the biotically effected air-sea flux by introducing a perfect virtual (unmeasurable in reality) tracer of production, remineralization and air-sea exchange (PRE). In the ocean interior, this tracer corresponds to the net sum of production and remineralization. Net surpluses or deficits of the virtual tracer reaching the sea surface are subject to air-sea exchange. In this

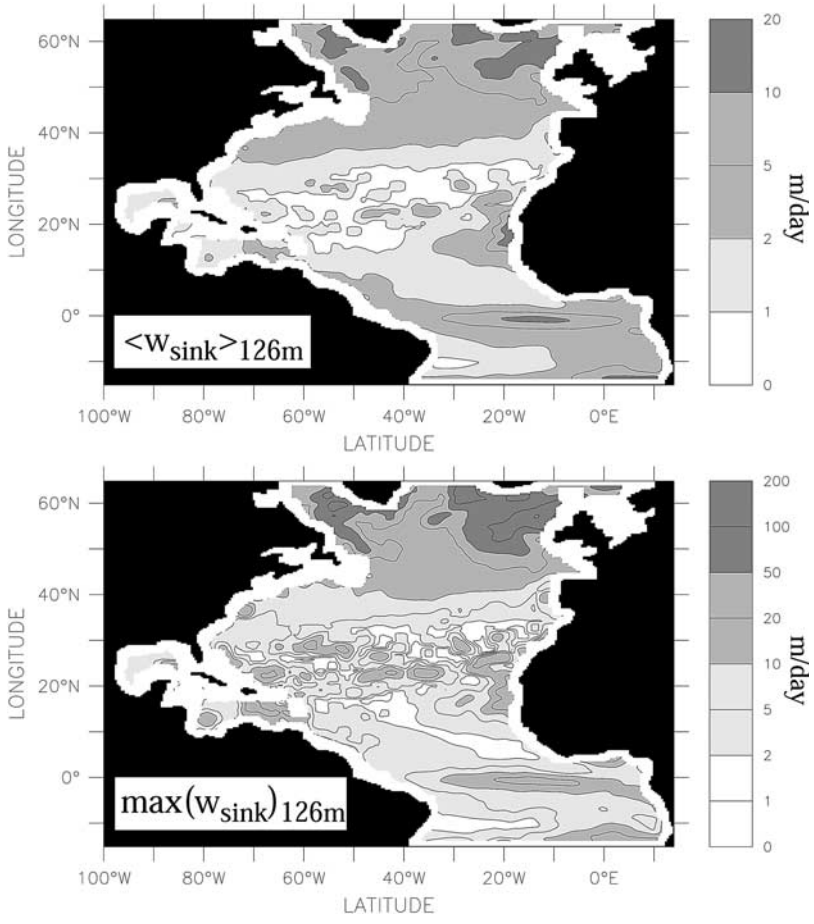

Figure 2. (top) Five-year mean sinking velocity of phytoplankton and detritus at 126 m depth as predicted by the particle aggregation model [*Kriest*, 2002] included in the ecosystem model. (bottom) Maximum sinking velocity simulated by the model at a depth of 126 m during the 5-year simulation period. The patchiness of sinking velocities in the subtropical gyre reflects individual small blooms, often related to mesoscale features which increase sinking velocities locally, including relatively small organic matter fluxes. Note the different scales in top and bottom panels.

respect, the PRE tracer acts like a gas dissolved in the ocean which is produced by remineralization and is consumed by primary production. In contrast to CO_2, however, the partial pressure of PRE is independent of temperature and carbonate chemistry. Thus it only describes the net effect of the biota on carbon distribution in the ocean and air-sea exchange.

[11] The PRE tracer is computed in nitrogen units (mmol N m^{-3}) and is initialized with zero concentration everywhere, so that to start with, it has no gradients on which mixing and circulation could act. Whenever the ecosystem model simulates uptake of nitrogen by phytoplankton, the analog of primary production, PRE is reduced by the corresponding amount. Whenever there is a nitrogen flux from phytoplankton, zooplankton, or detritus back into the DIN compartment, the analog of respiration, the concentration of PRE increases accordingly. Without air-sea exchange, PRE would thus record negative net community production (−NCP) within a water parcel.

[12] Air-sea exchange of the numerical PRE tracer is defined as follows: Atmospheric concentrations of PRE are constantly held at zero. This reflects complete equilibrium between ocean and atmosphere at initialization. Any gradient in PRE concentrations across the sea surface can only arise from PRE changes in the ocean. In the standard run, sea surface concentrations of PRE are restored to the atmospheric value of zero at each model time step; that is, we assume infinite dilution in an infinite atmosphere. With a model time step of 1 hour and a thickness of the upper layer of 11 m, this corresponds to a piston velocity of 11 m/hr. We refer to this rapid gas exchange as ''instantaneous'' and use the notation PRE_{inst}. The rapid air-sea exchange of PRE_{inst} is chosen in order to eliminate any impact of wind speed and of sea surface temperature and salinity, i.e., of physical properties. The effects of different parameterizations of the PRE tracer's air-sea exchange that are more appropriate for the description of real fluxes of gases will be discussed in section 6.

[13] Without biotic action, PRE concentrations would remain zero everywhere. It is only from primary production and respiration that tracer gradients develop which become subject to physical transport processes both across the air-

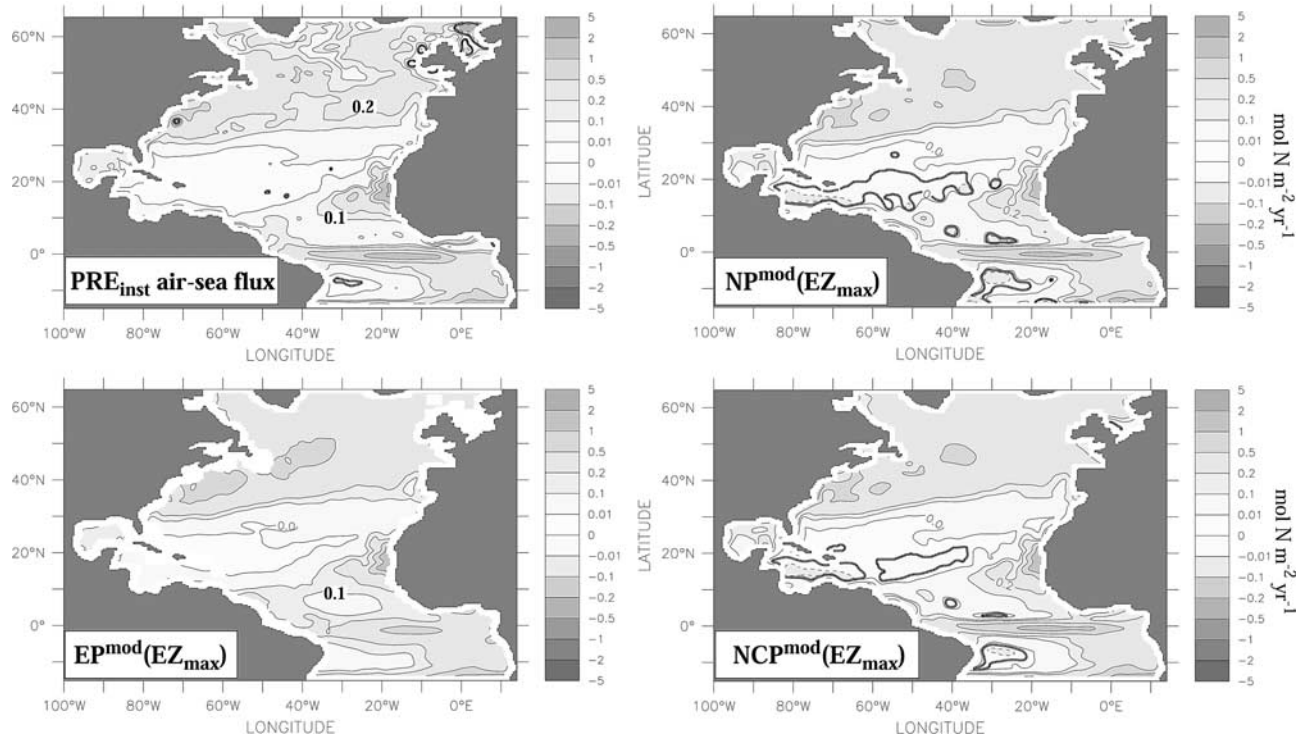

Figure 3. Five-year mean of the air-sea flux of the PRE_{inst} tracer (see text) representing the annual yield of the biological pump, of simulated new production (NP^{mod}_{EZmax}) above the maximum depth of the euphotic zone (EZ_{max}), of simulated export production (EP^{mod}_{EZmax}) by sinking, advection, and mixing across EZ_{max}, and of simulated annual net community production (NCP^{mod}_{EZmax}) above EZ_{max}. Unit is mol N m^{-2} yr^{-1}. See color version of this figure at back of this issue.

sea interface and within the water. Eventually, the tracer field should become qualitatively similar to the distribution of any nutrient or of DIC and finally reach steady state with all biotically and physically effected PRE transports compensating each other. To start with, we focus on the biotically effected air-sea flux of PRE during the first year after initialization of the PRE tracer. The PRE tracer is initialized at the end of winter (March 1) of each of the five successive years 16 to 20 of the coupled ecosystem-circulation model integration. Hence the simulated biology is in an approximate steady state for which the PRE tracer can measure the net impact of the marine biota on air-sea exchange. A year was chosen as the shortest steady-state period over which a comparison with NP, EP, and NCP is meaningful. The integral air-sea flux of PRE_{inst} of this first year after PRE initialization is considered as our reference value describing the (annual) yield of the biological pump. This is computed for each of the 5 years (16 to 20 of the coupled run), and the average of the five annual air-sea fluxes of PRE_{inst} (the yield of the biological pump) is shown in Figure 3. In accordance with the definition of the PRE tracer, the yield is computed in nitrogen units and can be converted into carbon or oxygen units by the Redfield ratio of the respective elements. Positive values of the air-sea flux of PRE reflect a positive yield of the biological pump, i.e., biotically effected uptake of carbon. Figure 3 shows that in our model, the marine biota act to generate oceanic carbon uptake essentially everywhere in the North Atlantic. Highest values are reached in the upwelling regions off West Africa and along the equator, and moderately high values in middle and high latitudes.

3.2. New Production

[14] Historically, new production (NP) was introduced as a measure of ecosystem yield [*Dugdale and Goering*, 1967]. It is defined as that portion of primary production fueled by new nitrogen supplied to, rather than nitrogen regenerated within, the euphotic zone. The depth level relevant for NP is thus clearly defined as the depth of the euphotic zone, operationally often taken as the depth of the 1% light level and typically varying from a few tens of meters in coastal waters to about 120 m in oligotrophic open-ocean regions. This definition leads to minor difficulties, since the depth of the euphotic zone varies in time, and for practical reasons a locally fixed depth level is employed instead. For our simulation, we choose the maximum depth of the euphotic zone reached during the annual cycle, EZ_{max} which varies between 120 m in the subtropics to about 90 m along the equator and at high latitudes (Figure 4a). The choice of a timescale required to distinguish "new" and "regenerated" nitrogen also remains problematic [*Platt et al.*, 1989], though an implicit annual timescale is generally assumed. Complying with its definition, new production is measured in nitrogen units.

[15] In our model, we use the total annual DIN supply into each $(1/3)^\circ \times (2/5)^\circ$ (approximately 35 × 35 km) grid-

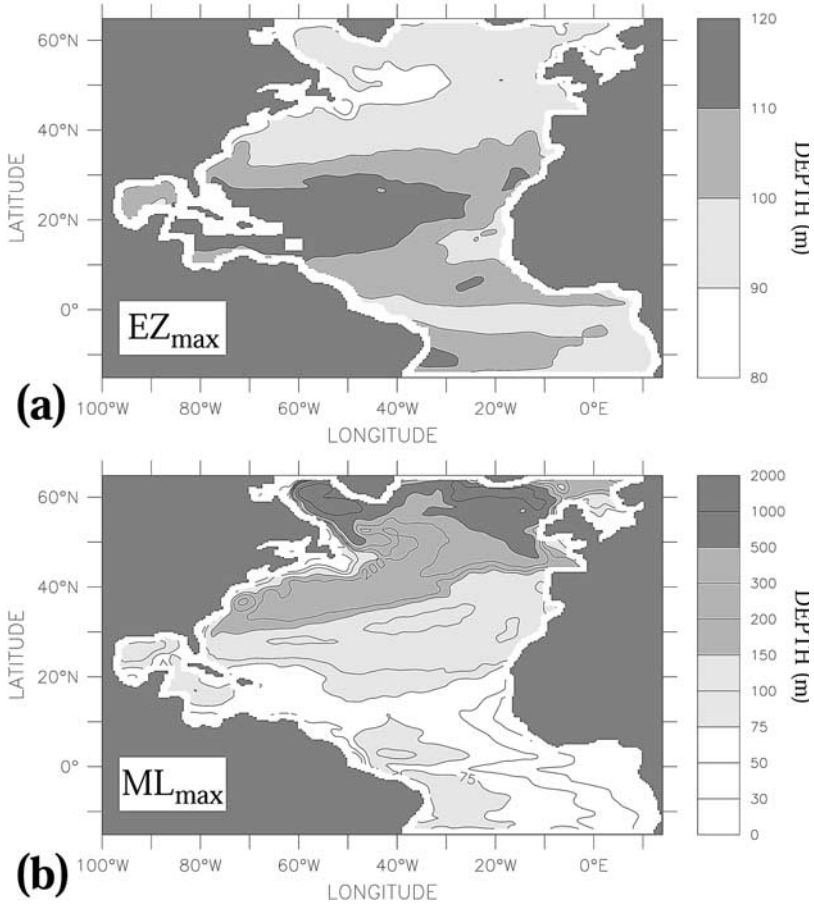

Figure 4. (a) Simulated maximum depth of the euphotic zone (1% light level) during the annual cycle, EZ_{max}. Both solar incidence angle and attenuation by phytoplankton are taken into account [*Oschlies and Garcon*, 1999]. (b) Simulated maximum depth of the mixed layer, ML_{max}, defined by a density criterion ($\Delta\sigma$ = 0.01 kg m^{-3}).

box column bounded by the sea surface and the maximum depth of the euphotic zone (EZ_{max}) as the model equivalent of new production, NP^{mod}_{EZmax}. A close equivalence with the original new production concept only holds for time intervals during which the DIN inventory within the euphotic zone stays constant, i.e., for annual and longer timescales in our steady-state model run. The spatial distribution of NP^{mod}_{EZmax} is shown in Figure 3. Although the euphotic zone is the reference depth constitutive of the NP concept, below we use the model equivalent of NP also with reference to the maximum depth of the surface mixed layer (indicated by the subscript MLmax).

3.3. Export Production

[16] A related, albeit less rigidly defined concept is that of export production (EP), which describes that fraction of primary production which is exported out of the surface layer. Commonly, the euphotic zone is chosen as the surface layer also for this concept. This has the advantage that in steady state, export production equals new production [*Eppley and Peterson*, 1979]. In fact, Eppley and Peterson still referred to new production, stating that the original definition by *Dugdale and Goering* [1967] (''the portion of total primary production that is available for higher trophic levels'') was ''quantitatively equivalent to the organic matter that can be exported from the total production in the euphotic zone without the production system running down.'' The distinct term ''export production'' is sometimes used for the particle export potentially collectable in sediment traps, and sometimes also accounts for export of suspended and dissolved material. With DOM not considered in our model, we here define EP^{mod}_{EZmax} as the total (particulate) organic-matter export across the maximum depth of the euphotic zone (Figure 3) in the form of sinking, passive advection, and mixing across the boundary. EP^{mod}_{EZmax} is computed in nitrogen units while EP is commonly given in carbon units.

3.4. Net Community Production

[17] Net community production (NCP) denotes the difference between gross primary production (GPP) and community respiration (R). With NCP positive, the volume under consideration is called net autotrophic and there is a net yield of organic matter which may either accumulate in, or be exported out of, the respective volume. In steady state, with no organic-matter accumulation, the yield of organic

Table 1. Simulated Annual Yield of the Biological Pump and Related Nitrogen Fluxes[a]

Flux, mol N m^{-2} yr^{-1}	EZ_{max}	ML_{max}
PRE_{inst} air-sea flux	0.1809 ± 0.0014	
NP^{mod}	0.2164 ± 0.0038	0.1729 ± 0.0051
EP^{mod}	0.2170 ± 0.0012	0.1729 ± 0.0020
NCP^{mod}	0.2158 ± 0.0012	0.1718 ± 0.0020
PRE_{inst} subduction	−0.0021 ± 0.0003	0.0140 ± 0.0010
PRE_{inst} vert.diff.	−0.0472 ± 0.0006	−0.0074 ± 0.0004
Accumulation:		
PRE_{inst}	0.0136 ± 0.0002	0.0020 ± 0.0001
DIN	−0.0017 ± 0.0020	−0.0001 ± 0.0035
PON	−0.0002 ± 0.0001	−0.0001 ± 0.0001
Spatial correlation with PRE_{inst}*air-sea flux*:		
NP^{mod}	0.84	0.88
EP^{mod}	0.64	0.34
NCP^{mod}	0.85	0.88

[a]Simulated air-sea flux of the PRE_{inst} tracer (see text), and simulated new production, NP^{mod}, export production, EP^{mod}, and net community production, NCP^{mod}. Results shown are averaged over the region 13°S–63°N of the North Atlantic and over a period of five years, with uncertainties given by the standard deviation of the five annual means. EZ_{max} is the maximum depth of the euphotic zone, and ML_{max} is the maximum depth of the mixed layer reached during the annual cycle. Subduction and vertical diffusion of PRE are positive for a PRE flux out of the respective layer. Whenever EZ_{max} or ML_{max} hit the ocean floor, an export across the respective surface cannot be computed (burial in the sediments is not accounted for in the model). Numbers for EP^{mod}, and subduction and vertical diffusion of PRE_{inst} across the respective depth surface are therefore scaled with the area of EZ_{max} ($47.38 \times 10^{12} m^2$) or ML_{max} ($47.41 \times 10^{12} m^2$) divided by the total surface area of the region 13°S–63°N ($49.83 \times 10^{12} m^2$). Small differences in the basin-average values for NP^{mod}, EP^{mod}, and NCP^{mod} arise from restoring to climatological nitrate fields at the closed lateral boundaries.

carbon equals its export. Unlike NP, the definition of NCP does not include a depth range and, in different contexts, NCP may refer to different volumes of water. To compare it with NP and EP, EZ_{max} is the appropriate depth.

[18] While NCP is commonly given in carbon units, we again use nitrogen units. In our model, NCP^{mod}_{EZmax} is primary production minus remineralization of phytoplankton, zooplankton, and detritus integrated over the depth of the euphotic zone (Figure 3).

4. Annual Timescale: Disparity of Concepts

4.1. Integral Considerations

[19] Under the simplifying assumptions that went into the model set-up (steady state, neglect of processes deviating from Redfield stoichiometry), the net input of DIN across the base of the euphotic zone (or any other depth level) must be balanced by net biological transformation of DIN into organic nitrogen and its subsequent export through the same depth level. This balance is reflected by the close agreement of the respective model-derived fluxes when integrated over the entire model domain (Table 1). However, the yield of the biological pump as estimated by the annual air-sea flux of PRE_{inst} amounts to only 0.181 mol N m^{-2} yr^{-1} (or 14.4 g C m^{-2} yr^{-1}) which is some 20% smaller than any of the biological production concepts when applied to the euphotic zone, i.e., NP^{mod}_{EZmax}, EP^{mod}_{EZmax}, or NCP^{mod}_{EZmax}. This discrepancy arises from the fact that air-sea exchange affects the surface mixed layer, not the euphotic zone. On annual and longer timescales, the maximum depth of the mixed layer is the appropriate depth level. On the basin average, this level is deeper (149 m) than the maximum depth of the euphotic zone (101 m) used for integration of the biological production rates (Figure 4). With respiration, but not production, extending to below the euphotic zone, NCP becomes smaller when integrated over a greater depth range. A more detailed analysis will follow below.

4.2. Regional Patterns

[20] Almost everywhere, PRE_{inst} is taken up by the ocean; that is, the yield of the biological pump is positive and there is biotically effected CO_2 uptake and O_2 release (Figure 3). Air-sea flux of PRE_{inst} is lowest (<0.01 mol N m^{-2} yr^{-1}) in the subtropics and highest (~1 mol N m^{-2} yr^{-1}) in the upwelling regions along the equator and off West Africa. On the basin scale, the biological production rates NP^{mod}_{EZmax}, EP^{mod}_{EZmax}, and NCP^{mod}_{EZmax} are similar to the PRE_{inst} air-sea flux, but a closer regional inspection reveals a number of systematic differences:

[21] • NP^{mod}_{EZmax} and NCP^{mod}_{EZmax} are negative, implying nitrate loss out of a net heterotrophic euphotic zone, over the southern part of the subtropical gyre as well as in small areas in the western part of the tropical Atlantic. Interestingly, both EP^{mod}_{EZmax} and air-sea flux of PRE_{inst} are positive in the same regions. Downward export of particulate organic matter (POM) out of net heterotrophic regions can be explained by convergent lateral advection of POM into the region [*Oschlies*, 2002]. Positive air-sea flux of PRE_{inst}, however, indicates that on the annual timescale, marine biology acts as a local sink of atmospheric CO_2 and as a source of O_2 even in these net heterotrophic areas. This is because the surface water which is in contact with the atmosphere is autotrophic in the annual mean. Figure 4 shows that the maximum mixed layer depth is shallower

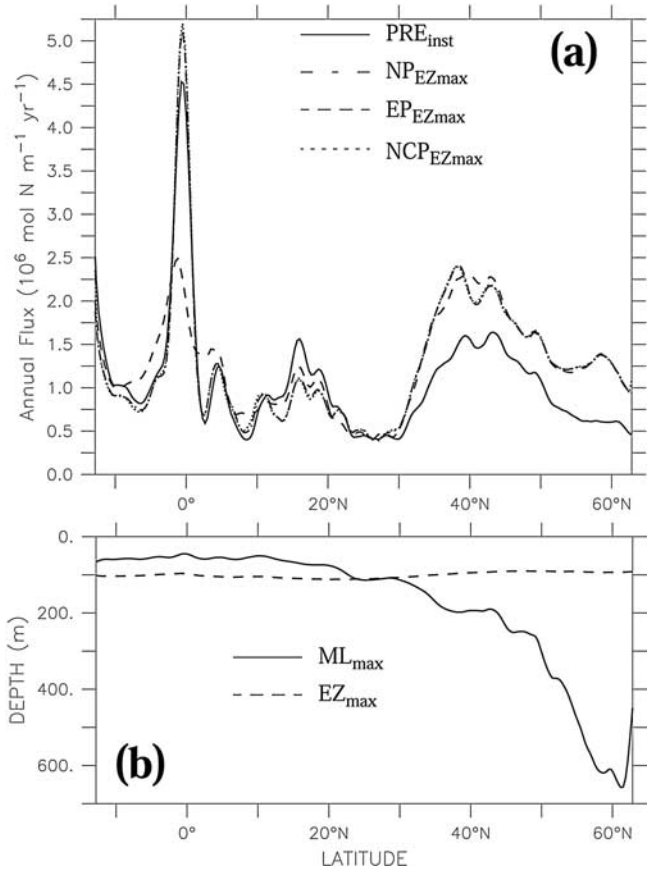

Figure 5. (a) Solid line: Zonally integrated air-sea flux of the PRE_{inst} tracer (see text). Dash-dotted line: Simulated new production (NP^{mod}_{EZmax}) above the maximum depth of the euphotic zone (EZ_{max}). Dashed line: Simulated export production (EP^{mod}_{EZmax}) across EZ_{max}. Dotted line: Simulated net community production (NCP^{mod}_{EZmax}) above EZ_{max}. (b) Zonally averaged annual-maximum depth of the euphotic zone, EZ_{max}, and zonally averaged maximum mixed-layer depth, ML_{max}.

than the depth of the euphotic zone in all areas for which the model predicts negative euphotic-zone NCP. Under these circumstances, and with NCP decreasing with depth, even regions with a net heterotrophic euphotic zone can have a biotically effected CO_2 uptake from, and O_2 release to, the atmosphere.

[22] • In the equatorial Atlantic, the air-sea flux of PRE_{inst}, NP^{mod}_{EZmax}, and NCP^{mod}_{EZmax} all show a relatively narrow maximum coinciding with equatorial upwelling. In contrast, the equatorial maximum in simulated EP^{mod}_{EZmax} is smaller in amplitude but extends over a wider meridional range, which is caused by the lateral transport of organic matter within the euphotic zone by the meridionally divergent flow field [*Oschlies*, 2002].

[23] • Over parts of the subpolar gyre, the air-sea flux of PRE_{inst} is considerably smaller (<0.1 mol N m^{-2} yr^{-1}) than the consistently high rates (>0.2 mol N m^{-2} yr^{-1}) of NP^{mod}_{EZmax}, EP^{mod}_{EZmax}, and NCP^{mod}_{EZmax}. This is also evident in the zonal integral which yields similar values for these three quantities all exceeding the zonally integrated PRE_{inst} air-sea flux by 30% to 50% north of 30°N (Figure 5a). In this region, the maximum depth of the mixed layer, ML_{max}, generally exceeds that of the euphotic zone, EZ_{max} (Figure 5b). The resulting greater integration depth leads to a decrease in integral NCP and yield of the biological pump.

5. Annual Timescale: Reconciliation of Concepts

5.1. A More Appropriate Depth Level

[24] The depth of the euphotic zone separates the water column into the light-lit surface layer and into the dark ocean beneath. It is, however, not the availability of light which is of immediate relevance to air-sea gas exchange, but material contact with the atmosphere. This condition is satisfied for the actual surface mixed layer. On annual and

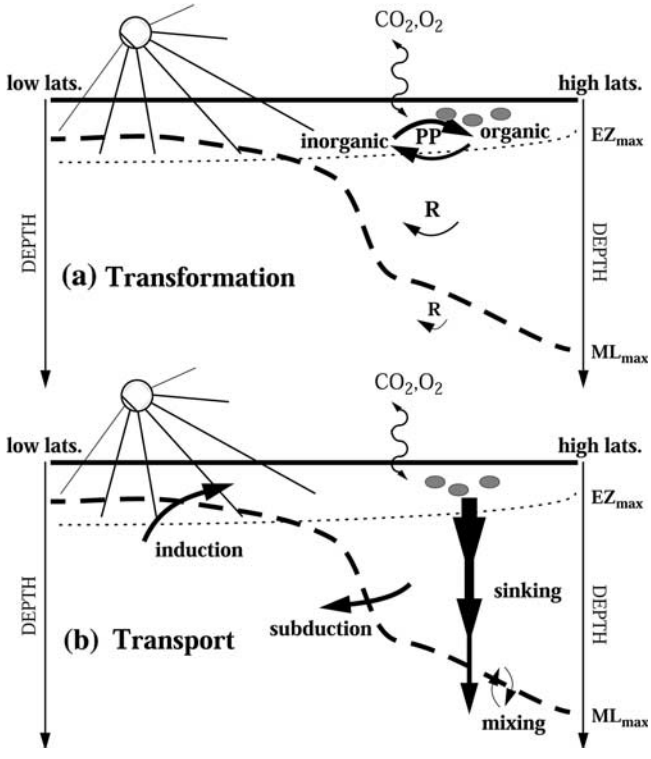

Figure 6. Schematic meridional section of the upper ocean. The dotted line denotes the maximum depth of the euphotic zone reached at each location during the annual cycle, EP_{max}. The thick dashed line represents the maximum depth of the mixed layer reached during the annual cycle, ML_{max}. The processes relevant for the yield of the biological pump are (a) transformation of inorganic to organic matter and back above the depth of the winter mixed layer, consisting of primary production (PP), which is confined to the euphotic zone, and respiration (R), which also can occur at depth; and (b) transport of biotically transformed matter across the depth of the winter mixed layer by sinking, mixing, subduction, and induction. As shown below, the transport relevant for biotically effected air-sea exchange also includes newly remineralized inorganic matter and newly generated inorganic-matter deficits.

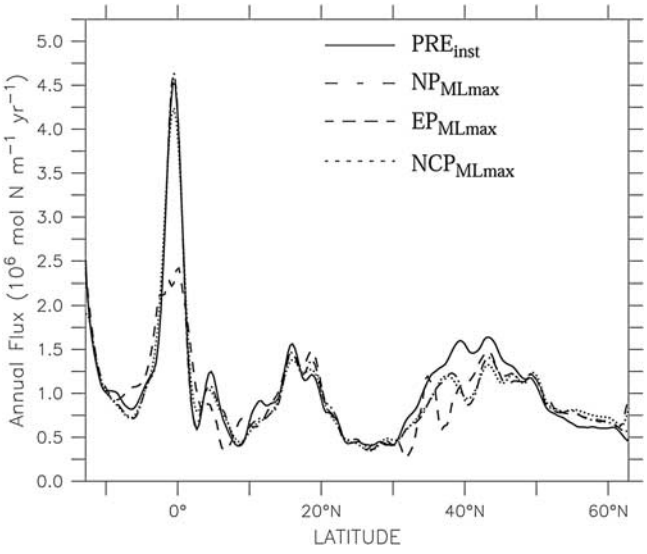

Figure 7. Solid line: Zonally integrated air-sea flux of the PRE_{inst} tracer (see text). Dash-dotted line: Simulated new production (NP^{mod}_{MLmax}) above the maximum mixed layer depth (ML_{max}). Dashed line: Simulated export production (EP^{mod}_{MLmax}) across the ML_{max} surface. Dotted line: Simulated net community production (NCP^{mod}_{MLmax}) above the ML_{max} surface.

longer timescales the relevant water volume in contact with the atmosphere is bounded from below by the maximum depth reached by the surface mixed layer during the annual cycle, usually the depth of the mixed layer in late winter. The situation is shown schematically in Figure 6 for a meridional section through the upper ocean. The maximum mixed-layer depth (ML_{max}) has a much larger meridional variability than the maximum depth of the euphotic zone (EZ_{max}). In general, ML_{max} is shallower than EZ_{max} in the tropics whereas it is several hundred meters deeper at high latitudes where deep and intermediate water masses form (see also Figures 4 and 5b).

[25] Overall agreement between NP^{mod}, EP^{mod}, and NCP^{mod} with the annual PRE_{inst} air-sea flux turns out to be considerably better when ML_{max} rather than EZ_{max} is chosen as the common reference level. This is evident in the zonal integral (compare Figure 7 and Figure 5a), but also holds for the regional distribution of the respective quantities (compare Figure 8 and Figure 3). Interestingly, in the model, none of the above biological production rates has any significant areas of negative values, for example, of net heterotrophy, when ML_{max} is used as the reference level.

[26] Although basin-averaged values of NP^{mod}_{MLmax}, EP^{mod}_{MLmax}, and NCP^{mod}_{MLmax} agree closely with each other, they are all still smaller by about 4% than the PRE_{inst} air-sea flux (Table 1). This small but significant (with respect to the errors in the budget calculations) discrepancy indicates some transport mechanism of biotically processed matter

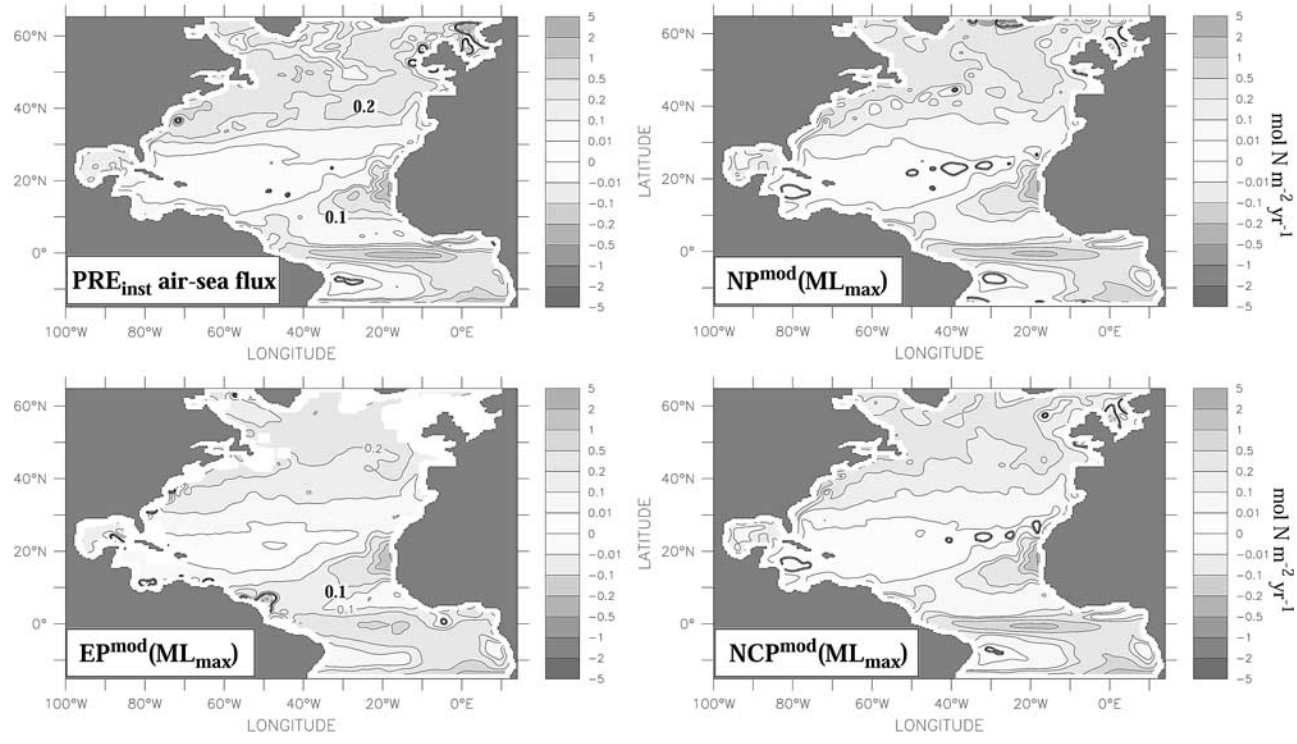

Figure 8. Five-year mean of the air-sea flux of the PRE_{inst} tracer (see text) representing the annual yield of the biological pump, of simulated new production (NP^{mod}_{MLmax}) above the maximum mixed layer depth (ML_{max}), of simulated export production (EP^{mod}_{MLmax}) across ML_{max}, and of simulated net community production (NCP^{mod}_{MLmax}) above ML_{max}. Unit is mol N m^{-2} yr^{-1}. See color version of this figure at back of this issue.

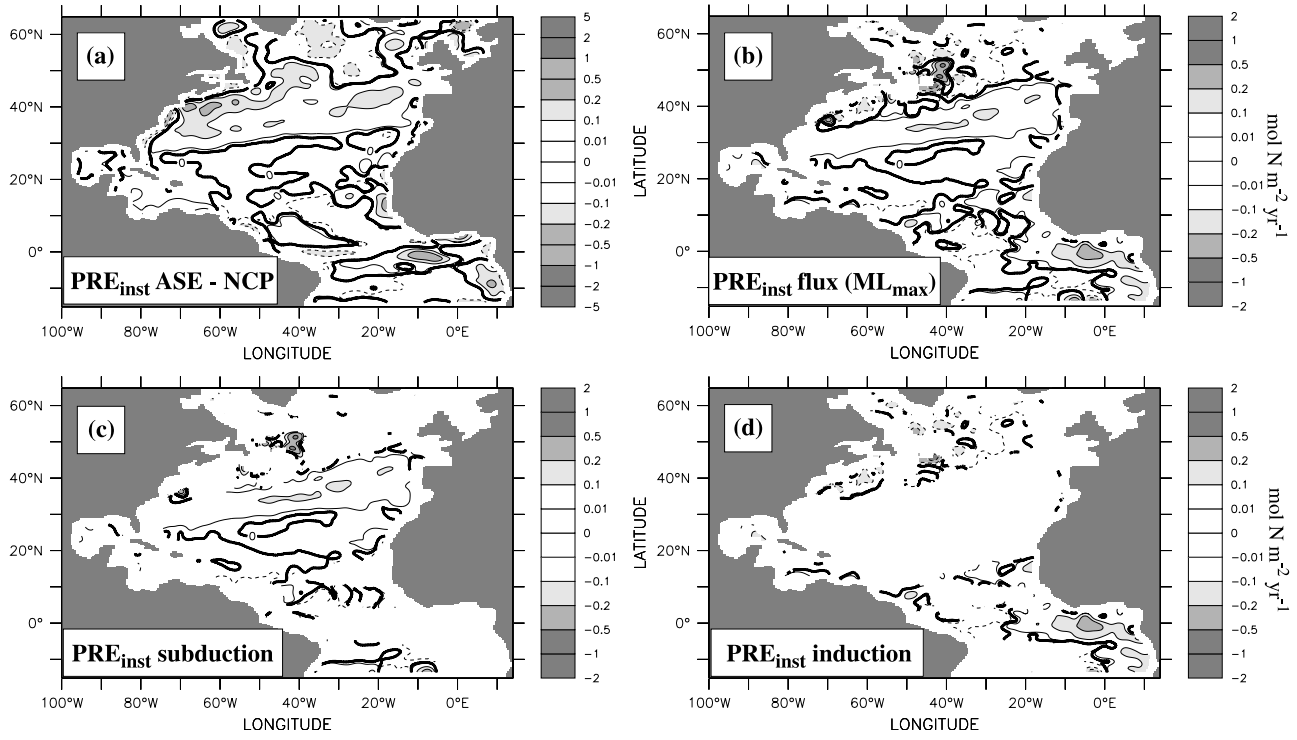

Figure 9. (a) Difference between simulated annual air-sea flux of the PRE_{inst} tracer (see text) and NCP above the maximum mixed layer depth (ML_{max}). (b) Annual transport of the PRE_{inst} tracer across ML_{max}. (c) Annual subduction of PRE_{inst} across ML_{max} in regions with positive subduction rates only. (d) Annual induction of PRE_{inst} across ML_{max} in regions with negative subduction rates only. Figure 9b is the superposition of Figures 9c and 9d. Unit is mol N m^{-2} yr^{-1}, and positive values in all panels indicate export of PRE_{inst} to below ML_{max} thereby increasing biotically effected air-sea fluxes of PRE_{inst} and, by inference, of CO_2. See color version of this figure at back of this issue.

relevant for air-sea gas exchange which is not accounted for in either of the biological rate concepts. The pattern of the difference between PRE_{inst} air-sea flux and NCP^{mod}_{MLmax} is shown in Figure 9a. In the subpolar North Atlantic, air-sea flux of PRE_{inst} is in general smaller than NCP^{mod}_{MLmax}, and the reverse is the case along an east-northeastwardly sloping band extending from the coast of Florida to the Iberian Peninsula.

5.2. Subduction of Newly Remineralized Inorganic Matter

[27] The maximum mixed layer depth, ML_{max}, is not a material boundary, and water can move across it. This process is termed subduction when water leaves the volume above ML_{max}. The reverse process, i.e. water entering the volume above ML_{max} from the thermocline, is termed induction. Water subduction or induction may occur both vertically and laterally by transport across a sloping ML_{max} surface. Induction usually supplies DIN to the water above ML_{max} and subduction contributes to the export of PON out of it. (In the present model, lateral subduction of PON contributes about 5% to the total PON export across ML_{max}.)

[28] In steady state, NP^{mod}_{MLmax} and EP^{mod}_{MLmax} are balanced and connected by NCP^{mod}_{MLmax} in the water volume above the ML_{max} surface. These biological rate concepts distinguish biogeochemical fluxes according to whether on passing through the ML_{max} surface the considered chemical element is in organic or inorganic form. However, this distinction is not relevant with respect to air-sea exchange. In particular, the actual surface mixed layer is shallower than ML_{max} during much of the growth season at middle and high latitudes as illustrated in Figure 10a. Part of the organic matter formed in, and exported out of, the actual surface mixed layer may subsequently be remineralized above ML_{max}. This was described above as causing the annual PRE_{inst} air-sea flux to be considerably smaller than NP^{mod}_{EZmax} at middle and high latitudes. Whenever this newly remineralized (and hence inorganic!) material is subducted across the ML_{max} surface, it will be shielded from contact with the atmosphere in the following winter (Figure 10a). In this way, this component thus has the same impact on the annual air-sea exchange as material exported as organic matter. This additional biotically effected drawdown by the subduction of newly remineralized inorganic matter can, in the model, be measured by the annual subduction of the PRE tracer across the ML_{max} surface. In reality, the subduction of newly remineralized inorganic matter can in principle be estimated from the subduction of apparent oxygen utilization (AOU).

[29] In our model, subduction of newly remineralized inorganic matter occurs mainly in an east-northeastwardly sloping band crossing the North Atlantic between Florida

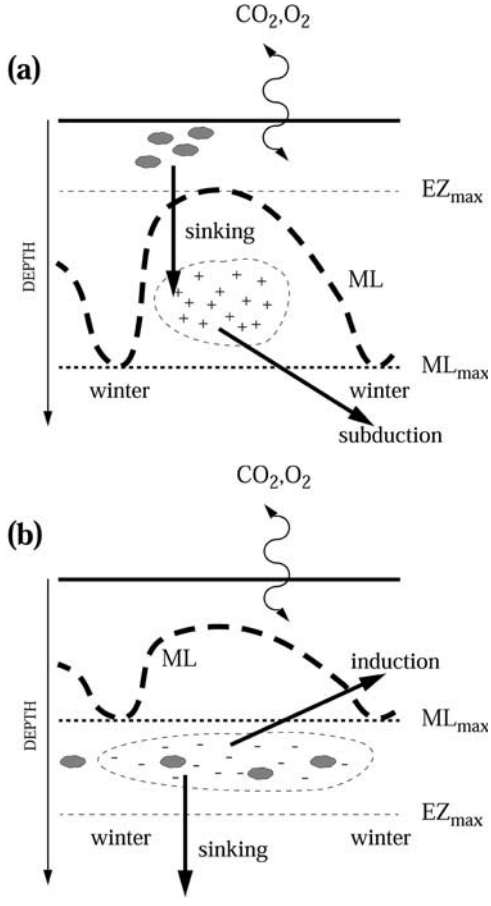

Figure 10. Typical temporal evolution of the seasonal surface mixed layer. (a) Subduction of newly remineralized inorganic matter across the maximum mixed layer depth (ML_{max}). (b) Induction of newly generated inorganic-matter deficits across ML_{max}.

and the Iberian Peninsula (Figure 9c). This band corresponds closely to the pronounced latitudinal slope in ML_{max} (Figure 4) which is also the region of mode water formation [*Marshall et al.*, 1993]. There, positive PRE_{inst} concentrations are subducted across the ML_{max} surface. The local contribution of the subduction of newly remineralized inorganic matter to the yield of the biological pump can exceed 0.1 mol N m^{-2} yr^{-1} or about 50%.

[30] Note, that in some regions like the southwestern part of the subtropical gyre, water is subducted with negative PRE_{inst} concentrations, which reflects the subduction of biotically generated inorganic-matter deficits out of the shallow (i.e., light-lit) seasonal thermocline above ML_{max} but below the actual mixed-layer base.

5.3. Induction of Newly Generated Inorganic-Matter Deficits

[31] A related process is the induction of newly generated inorganic matter deficits (Figure 10b): If ML_{max} is shallower than EZ_{max}, which is the case in large parts of the tropics and subtropics, net community production beneath ML_{max} can lower concentrations of inorganic nutrients and increase those of O_2. Entrainment of such waters into the actual surface mixed layer will contribute to the yield of the biological pump. In the model, this effect is measured as the induction of negative PRE concentrations. Note, that there may also be the induction of newly formed organic matter associated with the inorganic-matter deficit. This organic-matter flux is already accounted for in the above computation of EP^{mod}_{MLmax}.

[32] In our model, the induction of newly generated inorganic-matter deficits occurs mainly in the eastern part of the tropical Atlantic (Figure 9d) via upwelling of euphotic-zone water from below the ML_{max} surface. Over much of the subpolar North Atlantic the impact of induction on the yield of the biological pump is negative, because upwelling brings newly remineralized inorganic matter from the stratified thermocline back into atmospheric contact during a single annual cycle. Here the induction of newly remineralized inorganic matter explains why the yield of the biological pump can be lower than the biological rates (referenced to ML_{max}) by more than 0.1 mol N m^{-2} yr^{-1}.

[33] On basin average, subduction and induction of newly remineralized inorganic matter and of newly generated inorganic-matter deficits together contribute only 0.014 mol N m^{-2} yr^{-1}, or about 8%, to the total PRE_{inst} air-sea exchange (Table 1). Nevertheless, regional contributions can reach 50%, for example, in the midlatitude subduction band and in parts of the subpolar gyre. The diffusive upward flux of PRE across the ML_{max} level is relatively small (0.007 mol N m^{-2} yr^{-1}) with little regional variability. This is because ML_{max} is situated within the stratified thermocline throughout the year, and vertical diffusivities are persistently low there ($\sim$0.1 cm^2 s^{-1}).

6. Role of Time

6.1. Gas Exchange Velocity

[34] In the experiment discussed so far, air-sea gas exchange of the PRE_{inst} tracer was parameterized by restoring surface concentrations to atmospheric concentrations at every model time step of 1 hour, corresponding to a piston velocity of 11 m/hr. This is 1–2 orders of magnitude faster than typical gas-exchange velocities for gases like CO_2 or O_2. To examine the relation between the annual air-sea flux of the PRE_{inst} tracer and the biotically effected air-sea fluxes of CO_2 and O_2, two sensitivity experiments were performed: In one experiment, the PRE air-sea exchange velocity is taken equal to that of oxygen, with local piston velocities computed as a function of sea surface temperature (SST), sea surface salinity (SSS), and wind speed according to the OCMIP-2 protocol (R. G. Najjar and J. C. Orr, Design of OCMIP-2 simulations of chlorofluorocarbons, the solubility pump and common biogeochemistry, 1998; available from the World Wide Web at http://www.ipsl.jussieu.fr/OCMIP). This experiment is referred to as PRE_{fast}. To approximately account for the buffering capacity of the marine carbonate system which is not included in the present nitrogen-based model, a second sensitivity experiment was performed with a PRE_{slow} air-sea exchange velocity 10 times slower than that of PRE_{fast}. This reflects the fact that the average equilibration time of surface CO_2

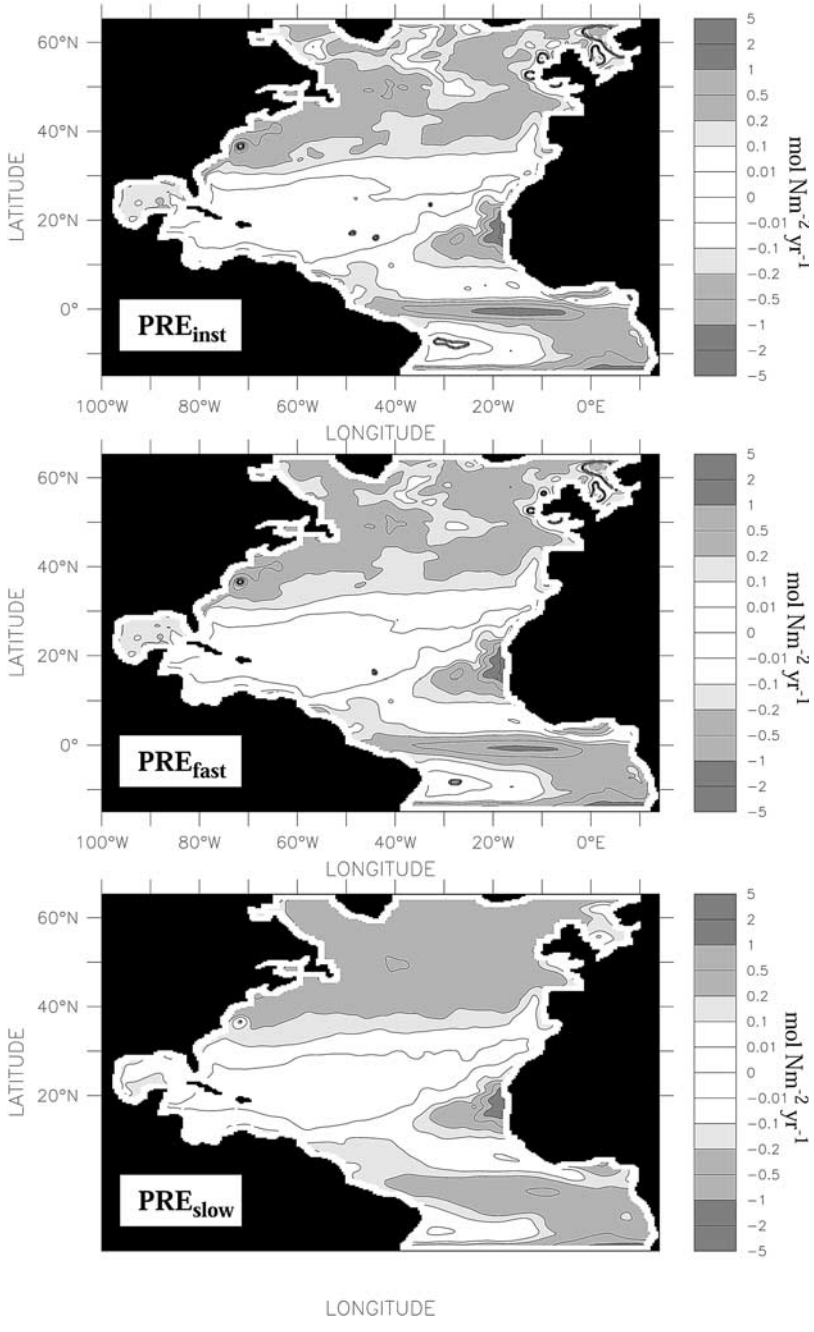

Figure 11. (top) Five-year mean of the simulated annual air-sea flux of the PRE_{inst} tracer (see text) for an air-sea exchange represented by restoring upper-layer concentrations to zero with a timescale of 1 hour (same as Figure 8a). (middle) Same as top panel, but with air-sea exchange represented by the piston velocity of oxygen (PRE_{fast}). (bottom) Same as middle panel, but with a 10 times slower air-sea equilibration (PRE_{slow}).

Table 2. Role of Air-Sea Gas Exchange Velocity

Flux, mol N m^{-2} yr^{-1}	PRE_{inst}	PRE_{fast}	PRE_{slow}
Air-sea flux	0.1809 ± 0.0014	0.1800 ± 0.0013	0.1731 ± 0.0014
Subduction of PRE across ML_{max}	0.0140 ± 0.0010	0.0154 ± 0.0009	0.0213 ± 0.0009
Vert.diffusion of PRE across ML_{max}	0.0074 ± 0.0004	0.0091 ± 0.0004	0.0140 ± 0.0005
Annual trend of PRE inventory (0-ML_{max})	0.0020 ± 0.0001	0.0016 ± 0.0001	−0.0011 ± 0.0002

with the atmosphere is larger than that of O_2 by a factor of about 10 [*Broecker and Peng*, 1982]. The annual air-sea flux of PRE_{slow} thus gives a coarse estimate of the biotically effected air-sea flux of CO_2.

[35] The differences between annual air-sea fluxes of PRE_{inst} and PRE_{fast} turn out to be small. Basin-mean fluxes differ by less than 1% (Table 2), and even regional patterns of PRE_{inst} and PRE_{fast} fluxes agree well with each other (Figure 11). This indicates that, in the present model run with monthly mean atmospheric forcing, the air-sea flux of O_2 across the sea surface is fast enough to keep up with biotically effected oxygen changes in the surface layer. It remains to be studied how a higher temporal resolution of atmospheric forcing would affect this conclusion.

[36] The average air-sea flux of PRE_{slow}, which approximates the biotically effected CO_2 exchange, turns out to be about 5% smaller than that of PRE_{inst} (Table 2) and reveals a spatial pattern considerably smoother than that of the air-sea exchange of PRE_{inst} or PRE_{fast} (Figure 11). The maximum of oceanic PRE uptake associated with the equatorial upwelling is less intense and extends over a wider latitudinal range for the slower gas exchange. Over the subpolar gyre, the air-sea flux of PRE_{slow} is everywhere larger than 0.2 mol N yr^{-1}, in contrast to small regions with values smaller than 0.1 mol N yr^{-1} in the PRE_{inst} run. Interestingly, subduction rates of PRE_{slow} are about 30% larger than those of PRE_{inst} (Table 2).

[37] Obviously, the sluggish exchange of PRE_{slow} with the atmosphere cannot keep up with the biotically effected seasonal changes in surface PRE concentrations. At the end of the annual cycle, surface concentrations of the PRE_{inst} and PRE_{fast} tracers (−0.0004 mmol N m^{-3} and −0.01 mmol N m^{-3}, respectively) are relatively close to the atmospheric value of zero, whereas surface values of PRE_{slow} amount to −0.33 mmol N m^{-3}. Since beginning and end of the annual cycle were chosen to be in late winter (March 1), which is also the time of water mass formation [*Williams et al.*, 1995], differences among PRE_{fast} and PRE_{slow} concentrations at the end of the annual cycle reveal different effects of the previous year's biology on preformed values of O_2 and DIC. (Note the consequences for the interpretation of nutrient and CO_2 parameters derived from AOU.)

6.2. Yield of the Biological Pump on Annual and Decadal Timescales

[38] In a seasonal ocean, 1 year is the shortest relevant period for a steady-state concept of the biological pump. To measure its annual yield, the PRE tracer was reset to zero concentrations at the end of each winter in the above experiments.

[39] On timescales much longer than the annual cycle, essentially all of the material originally transformed by the marine biota and exported across the maximum mixed-layer depth will return to the surface layer as remineralized inorganic matter. The time lag of this return depends on the intensity of ocean circulation and the depth reached by the export. This was studied in an additional experiment during which the PRE tracer was not reset to zero each winter. The temporal evolution of the resulting PRE_{inst}, PRE_{fast}, and PRE_{slow} air-sea fluxes for a 25-year period is shown in Figure 12. The air-sea fluxes of PRE_{inst} and PRE_{fast} are highest in the first year, whereas the slower equilibration of the PRE_{slow} tracer with the atmosphere results in maximum PRE_{slow} air-sea fluxes in the second year. Irrespective of the gas exchange velocity, annual air-sea exchange of PRE decreases by 40–50% in 25 years. The reason for this decrease is that, given more time, older water with a larger inventory of accumulated respiration products reaches the air-sea interface. A similar decrease can be deduced from the simulated temporal evolution of the oceanic CO_2 loss in a global model after a complete shutdown of marine life [*Maier-Reimer et al.*, 1996].

[40] To estimate the biotically effected air-sea flux of CO_2 and O_2 on the decadal timescale, the air-sea flux of PRE is shown for year 10 of the experiments run without resetting

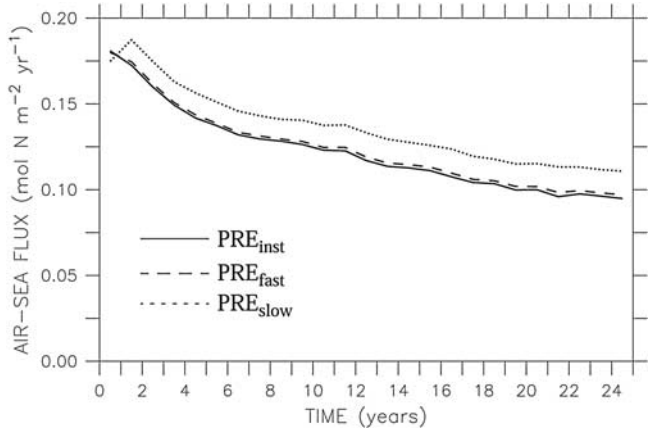

Figure 12. Temporal evolution of the annual air-sea flux of the PRE tracers for a 25-year simulation run without resetting concentrations to zero each winter. The solid line refers to restoring surface concentrations to atmospheric values at each model time step (PRE_{inst}), the dashed line which almost coincides with the solid line refers to a PRE air-sea exchange at the speed of oxygen (PRE_{fast}), and the dotted line refers to an air-sea exchange 10 times slower than that of oxygen (PRE_{slow}).

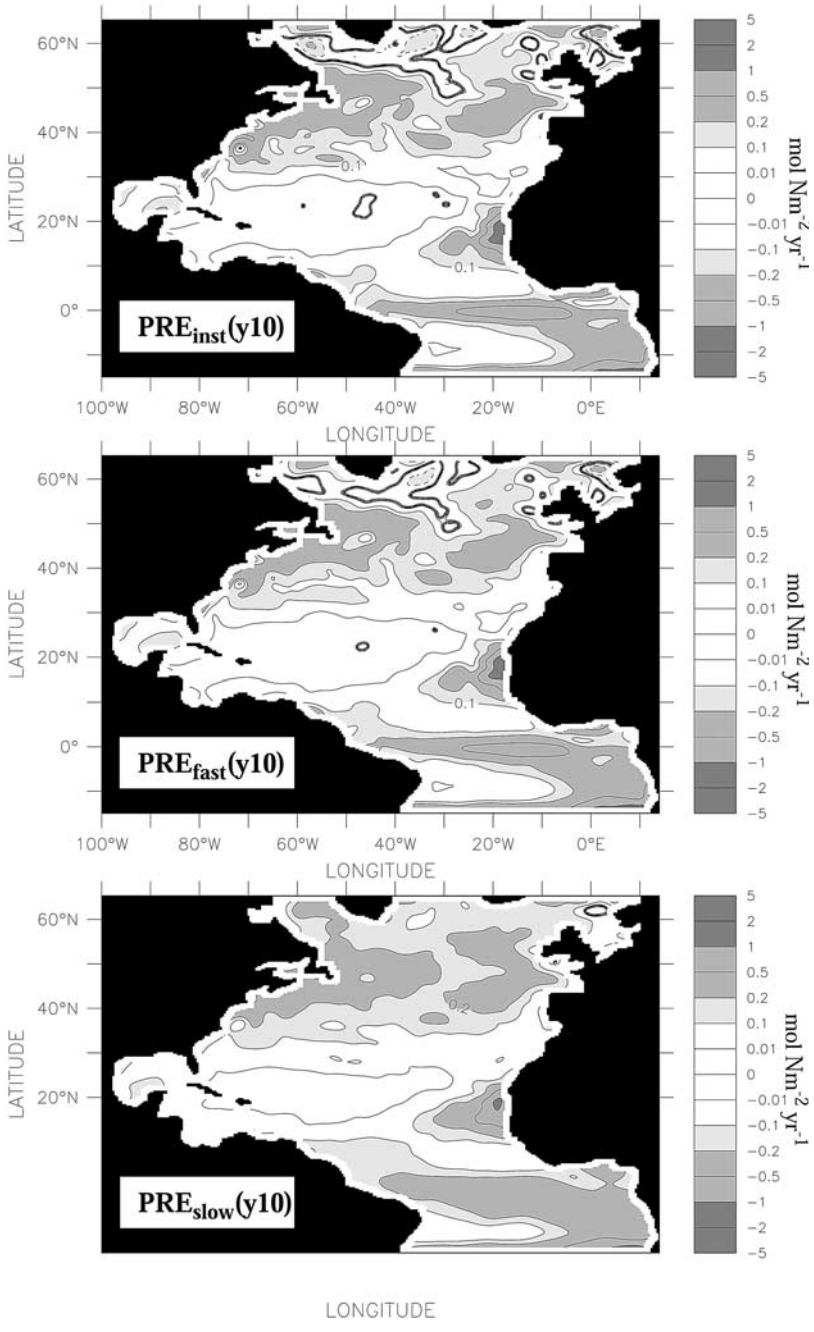

Figure 13. Simulated air-sea fluxes of the PRE tracer (see text) of year 10 after initialization with zero PRE concentrations. (top) PRE_{inst} tracer for an air-sea exchange represented by restoring upper-layer concentrations to zero with a timescale of 1 hour. (middle) PRE_{fast} tracer with air-sea exchange represented by the piston velocity of oxygen. (bottom) PRE_{slow} tracer with air-sea exchange 10 times slower than that of PRE_{fast}.

PRE concentrations to zero each winter (Figure 13). Interestingly, over parts of the subpolar North Atlantic the biological pump leads to outgassing of both the PRE_{inst} and PRE_{fast} tracers on this timescale. At the same time, PRE_{slow} still shows an air-sea flux directed into the ocean essentially everywhere. These results indicate that changes in biological production (here assuming no changes in the ocean circulation) may, on the decadal timescale, even generate transient changes in the air-sea fluxes of CO_2 and (minus) O_2 of opposite sign. According to our model results, increasing biological production would temporally increase oceanic CO_2 uptake but decrease O_2 release over part of the subpolar North Atlantic. On timescales longer than a few decades, the biological pump decreases both O_2 release and CO_2 uptake over large parts of the subpolar North Atlantic. When integrating a global model to equilibrium, *Toggweiler et al.* [2003] also found that on very long timescales the biological pump leads to an outgassing of CO_2 over the subpolar North Atlantic. This outgassing balances the biotically effected uptake of CO_2 elsewhere such that, in equilibrium and neglecting burial in sediments and riverine and atmospheric carbon inputs, the global air-sea flux of CO_2 associated with the biological pump becomes zero.

7. Summary and Conclusions

[41] In this paper we have investigated the biotically effected air-sea fluxes of CO_2 and O_2 in a simplified but consistent model framework, leaving out any special processes like nitrogen fixation, denitrification, formation of carbon-rich organic matter, and calcification, and employing constant Redfield stoichiometry throughout. The biotically effected drawdown of surface nutrients and surface DIC is the delivery rate or yield of the biological pump which, as a rate, contrasts the concentration-based concept of the strength of the biological pump [*Volk and Hoffert*, 1985]. To quantify the yield of the biological pump, a new tracer, "production, remineralization and air-sea exchange" (PRE) was defined such that the air-sea flux of PRE is the biological pump's yield. The PRE tracer is computed in nitrogen units and can be converted to carbon or oxygen via the appropriate conversion factors. There is no precise counterpart of this tracer which can be observed in the real ocean; the closest observable analog is changes in apparent oxygen utilization (i.e., oxygen utilization rate, OUR).

[42] Note that the lack of a direct method to practically measure the PRE tracer in all circumstances is not unique to it. The three rate concepts (NP, EP, NCP) give rise to similar problems. As soon as they are measured, many of their theoretical foundations and boundary conditions may be violated. For NP, we already pointed out the practical difficulty of determining the extent of the euphotic zone. The uptake of nitrate in experiments or calculated from seasonal differences of nitrate stocks is not exclusively a measure of new production. Both the nitrate source (part of the nitrate may be seasonally regenerated [*Koeve*, 2001; *Lipschultz*, 2001]) and its sink (uptake of nitrate by heterotrophs [*Bronk et al.*, 1994]) include components which are not consistent with new production's definition. Similar discrepancies between concepts and practical applications exist for NCP regarding the inclusion or not of effects of DOC [*Hansell and Carlson*, 1998], and for EP regarding the practical difficulties with measuring EP using sediment traps [*Gust et al.*, 1994; *Gardner*, 2000; *Kähler and Bauerfeind*, 2001].

[43] When comparing the yield of the biological pump with the biological production rates in the model, we were able to avoid such difficulties and to assess how well the biological rate concepts may work in the context of air-sea gas exchange. While we anticipate that the outcome of our study will be subject to modifications once the dynamics of the non-Redfield processes not considered here are taken into account, some general conclusions can already be derived from the work presented here:

[44] • The yield of the biological pump, i.e. the biotically effected air-sea flux of PRE, turns out to be about 16% smaller than the model-derived values of new production, export production, and net community production when, according to common practice, these biological rate concepts are applied to the euphotic zone. At the same time, the yield is positive essentially everywhere, even in those regions of the subtropical North Atlantic for which the model simulates a net heterotrophic euphotic zone. Obviously, biological production rates within the euphotic zone are unsuitable as estimates of the amount (in cases even of the direction) of the biotically effected air-sea fluxes of CO_2 or O_2.

[45] • Agreement between biological production concepts and the yield of the biological pump, i.e., the biotically effected air-sea exchange, becomes much better when, instead of the euphotic zone, the maximum depth reached by the surface mixed layer during the annual cycle, ML_{max}, is used as the reference level. This is because the relevant property for air-sea exchange is not the availability of light, but material contact with the atmosphere. In a basin-scale analysis of sediment trap data, *Koeve* [2002] estimated that about 15% of the particulate organic matter (POM) sinking out of the euphotic zone was remineralized above the ML_{max} level. In our model, about 10% of the POM sinking out of the euphotic zone (0.195 mol N m^{-2} yr^{-1}) and about 20% of the total organic matter export EP^{mod} (which includes advective and turbulent POM transports) is remineralized in this depth range (Table 1).

[46] • Even when ML_{max} is used as reference depth, substantial discrepancies between biological production rates and the biotically effected air-sea exchange remain. These discrepancies arise from the fact that the biological rate concepts partition biogeochemical fluxes into fluxes of organic and of inorganic matter whereas, for air-sea exchange, it is not relevant whether the material, on crossing the ML_{max} surface, is in organic or inorganic form. To reconcile biological rate concepts and biotically effected air-sea exchange, inorganic contributions to the biological pump must also be accounted for. These include the subduction of newly remineralized inorganic matter and induction of newly formed inorganic-matter deficits across the ML_{max} surface. On the basin average, this contributes only about 8% of the biotically effected air-sea exchange, but local contributions may be much larger: In the mode-

water source regions along the east-northeastwardly sloping band of poleward deepening winter mixed layers, subduction of newly remineralized inorganic matter accounts for about half of the simulated biotically effected air-sea fluxes of CO_2 and O_2. These are also the areas of the ocean where, on annual and longer timescales, the export of DOM takes place [*Doval and Hansell*, 2000; P. Kähler et al., unpublished manuscript, 2003]. Also, for this export, the distinction between DOC and its inorganic remineralization product (CO_2) is meaningless in terms of carbon air-sea exchange.

[47] • The inorganic contribution to the biological pump via subduction and induction processes may allow for wind-driven and relatively rapid changes in biotically effected air-sea fluxes via changes in subduction rates. As the water masses subducted into the main thermocline are shielded from atmospheric contact typically for a few decades, this may particularly affect interannual to decadal variations in the air-sea fluxes of CO_2 and O_2. Moreover, changes of the maximum depth of the mixed layer may generate large changes in the yield of the biological pump with relatively small changes in the biological production rates.

[48] • Different equilibration times of CO_2 and O_2 with the atmosphere result in different response times of the respective biotically effected air-sea fluxes to changes in the marine biology. The model results indicate that over parts of the subpolar North Atlantic the biotically effected variations in air-sea fluxes of CO_2 and (minus) O_2 can have opposite phases on decadal timescales. This is relevant for attempts to infer temporal variation in the air-sea flux of CO_2 from the atmospheric O_2/N_2 ratio [*Keeling et al.*, 1996].

[49] **Acknowledgments.** We thank Wolfgang Koeve, Karin Lochte, and an anonymous reviewer for very helpful and constructive comments.

References

Barnier, B., L. Siefridt, and P. Marchesiello (1995), Surface thermal boundary condition for a global ocean circulation model from a three-year climatology of ECMWF analyses, *J. Mar. Syst.*, *6*, 363–380.

Broecker, W. S., and T. H. Peng (1982), *Tracers in the Sea*, Eldigio, Palisades, N. Y.

Bronk, D. A., P. M. Glibert, and B. B. Ward (1994), Nitrogen uptake, dissolved organic nitrogen release, and new production, *Science*, *265*, 1843–1845.

del Giorgio, P. A., J. J. Cole, and A. Cimbleris (1997), Respiration rates in bacteria production exceed phytoplankton production in unproductive aquatic systems, *Nature*, *385*, 148–151.

Doval, M. D., and D. A. Hansell (2000), Organic carbon and apparent oxygen utilization in the western South Pacific and the central Indian Ocean, *Mar. Chem.*, *68*, 249–264.

Dugdale, R. C., and J. J. Goering (1967), Uptake of new and regenerated forms of nitrogen in marine production, *Limnol. Oceanogr.*, *12*, 196–206.

Eppley, R. W., and B. J. Peterson (1979), Particulate organic matter flux and planktonic new production in the deep ocean, *Nature*, *282*, 677–680.

Gardner, W. D. (2000), Sediment trap technology and sampling in surface waters, in *The Changing Ocean Carbon Cycle: A Midterm Synthesis of the Joint Global Ocean Flux Study*, edited by R. B. Hanson, H. W. Ducklow, and J. G. Field, pp 240–281, Cambridge Univ. Press, New York.

Gaspar, P., Y. Gregoris, and J.-M. Lefevre (1990), A simple eddy kinetic energy model for simulations of the oceanic vertical mixing: Tests at station Papa and Long-Term Upper Ocean Study site, *J. Geophys. Res.*, *95*, 16,179–16,193.

Gibson, J. K., P. Kallberg, S. Uppala, A. Hernandez, A. Nomura, and E. Serrano (1997), ECMWF re-analysis project report series, vol. 1, ERA Description, report, 72 pp., Eur. Cent. for Medium-Range Weather Forecasting, Reading, UK.

Gust, G., A. F. Michaelis, R. Johnson, W. G. Deuser, and W. Bowles (1994), Mooring line motions and sediment trap hydromechanics: In situ intercomparison of three common deployment designs, *Deep Sea Res., Part I*, *41*, 5–6.

Haney, R. L. (1971), Surface thermal boundary condition for ocean circulation models, *J. Phys. Oceanogr.*, *1*, 241–248.

Hansell, D. A., and C. A. Carlson (1998), Net community production of dissolved organic carbon, *Global Biogeochem. Cycles*, *12*, 443–453.

Jenkins, W. J. (1982), Oxygen utilization rates in North Atlantic subtropical gyre and primary production in oligotrophic systems, *Nature*, *300*, 246–248.

Kähler, P., and E. Bauerfeind (2001), Organic particles in a shallow sediment trap: Substantial loss to the dissolved phase, *Limnol. Oceanogr.*, *46*, 719–723.

Keeling, R. F., S. C. Piper, and M. Heimann (1996), Global and hemispheric CO_2 sinks deduced from changes in atmospheric O_2 concentration, *Nature*, *381*, 218–221.

Koeve, W. (2001), Wintertime nutrients in the North Atlantic: New approaches and implications for new production estimates, *Mar. Chem.*, *74*, 245–260.

Koeve, W. (2002), Upper ocean carbon fluxes in the Atlantic Ocean: The importance of the POC:PIC ratio, *Global Biogeochem. Cycles*, *16*(4), 1956, doi:10.1029/2001GB001836.

Kriest, I. (2002), Different parameterizations of marine snow in a 1D-model and their influence on representation of marine snow, nitrogen budget and sedimentation, *Deep Sea Res., Part I*, *49*, 2133–2162.

Kriest, I., and G. T. Evans (1999), Representing phytoplankton aggregates in biogeochemical models, *Deep Sea Res., Part I*, *46*, 1841–1859.

Ledwell, J. R., A. J. Watson, and C. S. Law (1993), Evidence for slow mixing across the pycnocline from an open-ocean tracer-release experiment, *Nature*, *364*, 701–703.

Ledwell, J. R., A. J. Watson, and C. S. Law (1998), Mixing of a tracer in the pycnocline, *J. Geophys. Res.*, *103*, 21,499–21,529.

Levitus, S., R. Burgett, and T. P. Boyer (1994), World Ocean Atlas 1994, vol. 3, *Salinity, NOAA Atlas NESDIS 3*, 99 pp., Natl. Oceanic and Atmos. Admin., Silver Spring, Md.

Lipschultz, F. (2001), A time-series assessment of the nitrogen cycle at BATS, *Deep Sea Res., Part II*, *48*, 1897–1924.

Maier-Reimer, E., U. Mikolajewicz, and A. Winguth (1996), Future ocean uptake of CO_2: Interaction between ocean circulation and biology, *Clim. Dyn.*, *12*, 711–721.

Marshall, J. C., A. J. G. Nurser, and R. G. Williams (1993), Inferring the subduction rate and period over the North Atlantic, *J. Phys. Oceanogr.*, *23*, 1315–1329.

Oschlies, A. (2002), Nutrient supply to the surface waters of the North Atlantic: A model study, *J. Geophys. Res.*, *107*(C5), 3046, doi:10.1029/2000JC000275.

Oschlies, A., and V. Garçon (1999), An eddy-permitting coupled physical-biological model of the North Atlantic: I. Sensitivity to advection numerics and mixed layer physics, *Global Biogeochem. Cycles*, *13*, 135–160.

Oschlies, A., W. Koeve, and V. Garçon (2000), An eddy-permitting coupled physical-biological model of the North Atlantic: II. Ecosystem dynamics and comparison with satellite and JGOFS local studies data, *Global Biogeochem. Cycles*, *14*, 499–523.

Pacanowski, R., K. Dixon, and A. Rosati (1991), The G. F. D.L Modular Ocean Model users guide version 1, *Tech. Rep. 2*, GFDL Ocean Group, Geophys. Fluid Dyn. Lab., Princeton, N. J.

Platt, T., W. G. Harrison, M. R. Lewis, W. K. W. Li, S. Sathyendranath, R. E. Smith, and A. F. Vezina (1989), Biological production in the oceans: The case for a consensus, *Mar. Ecol. Prog. Ser.*, *52*, 77–88.

Prentice, I. C., G. D. Farquhar, M. J. R. Fasham, M. L. Goulden, M. Heimann, V. J. Jaramillo, H. S. Kheshgi, C. Le Quéré, R. J. Scholes, and D. W. R. Wallace (2001), The carbon cycle and atmospheric carbon dioxide, in *Climate Change 2001: The Scientific Basis, Contribution of Working Group I to the Third Assessment Report of the Intergovernmental Panel on Climate Change*, edited by J. T. Houghton et al., pp. 183–237, Cambridge Univ. Press, New York.

Sambrotto, R. N., G. Savidge, C. Robinson, P. Boyd, T. Takahashi, D. M. Karl, C. Langdon, D. Chipman, J. Marra, and L. Copispoti (1993), Elevated consumption of carbon relative to nitrogen in the surface ocean, *Nature*, *363*, 248–250.

Sarmiento, J. L., and U. Siegenthaler (1992), New production and the global carbon cycle, in *Primary Productivity and Biogeochemical Cycles in the Sea*, edited by P. Falkowski and A. D. Woodhead, pp. 317–332, Plenum, New York.

Toggweiler, J. R., A. Gnanadesikan, S. Carson, R. Murnane, and J. L. Sarmiento (2003), Representation of the carbon cycle in box models

and GCMs: 2. Organic pump, *Global Biogeochem. Cycles*, *17*(1), 1027, doi:10.1029/2001GB001841.

Volk, T., and M. I. Hoffert (1985), Ocean carbon pumps: Analysis of relative strengths and efficiencies in ocean-driven atmospheric CO_2 changes, in *The Carbon Cycle and Atmospheric CO_2: Natural Variations, Archean to Present*, *Geophys. Monogr. Ser.*, vol. 32, edited by E. Sundquist and W. Broecker, pp. 99–110, AGU, Washington, D. C.

Williams, P. J. L. B. (1993), On the definition of plankton production terms, *ICES Mar. Sci. Symp.*, *197*, 9–19.

Williams, R. G., M. A. Spall, and J. C. Marshall (1995), Does Stommel's mixed layer "demon" work?, *J. Phys Oceanogr.*, *25*, 3089–3102.

P. Kähler and A. Oschlies, Institut für Meereskunde an der Universität Kiel, Düsternbrooker Weg 20, 24105 Kiel, Germany. (pkaehler@ifm.uni-kiel.de; aoschlies@ifm.uni-kiel.de)

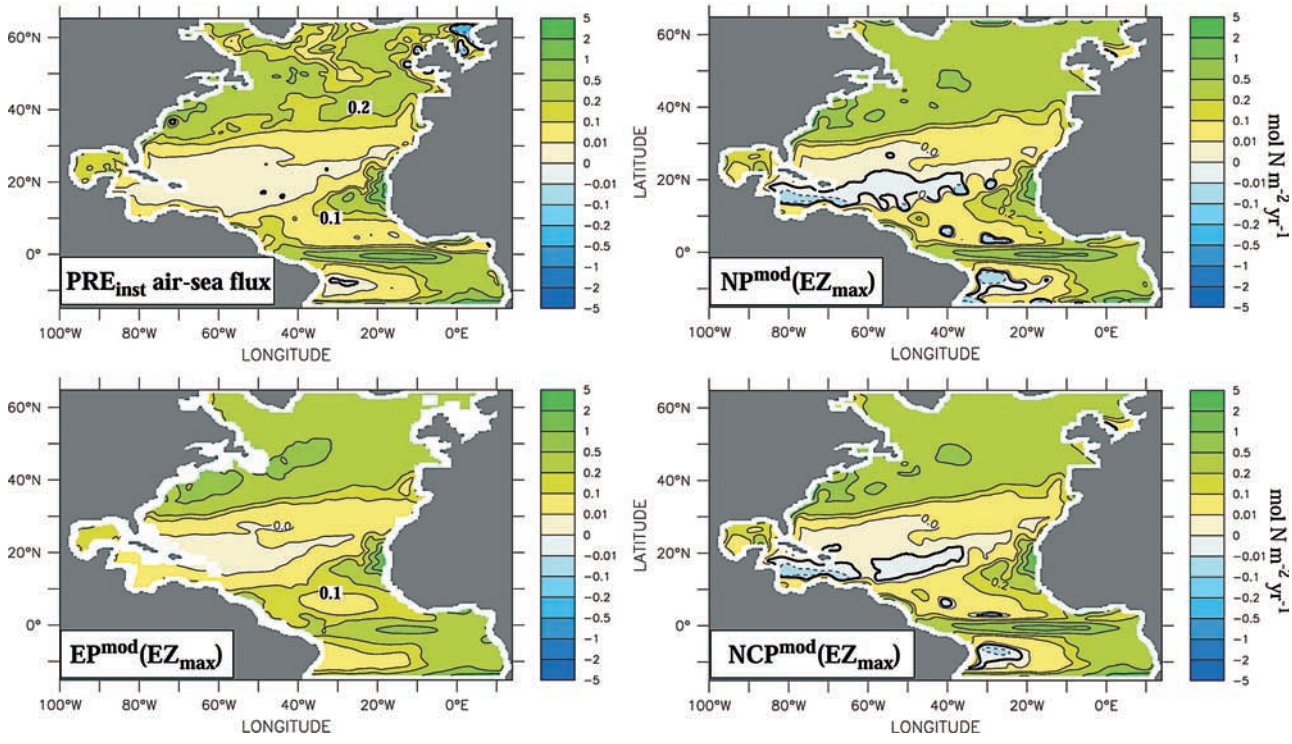

Figure 3. Five-year mean of the air-sea flux of the PRE_{inst} tracer (see text) representing the annual yield of the biological pump, of simulated new production (NP^{mod}_{EZmax}) above the maximum depth of the euphotic zone (EZ_{max}), of simulated export production (EP^{mod}_{EZmax}) by sinking, advection, and mixing across EZ_{max}, and of simulated annual net community production (NCP^{mod}_{EZmax}) above EZ_{max}. Unit is mol N m^{-2} yr^{-1}.

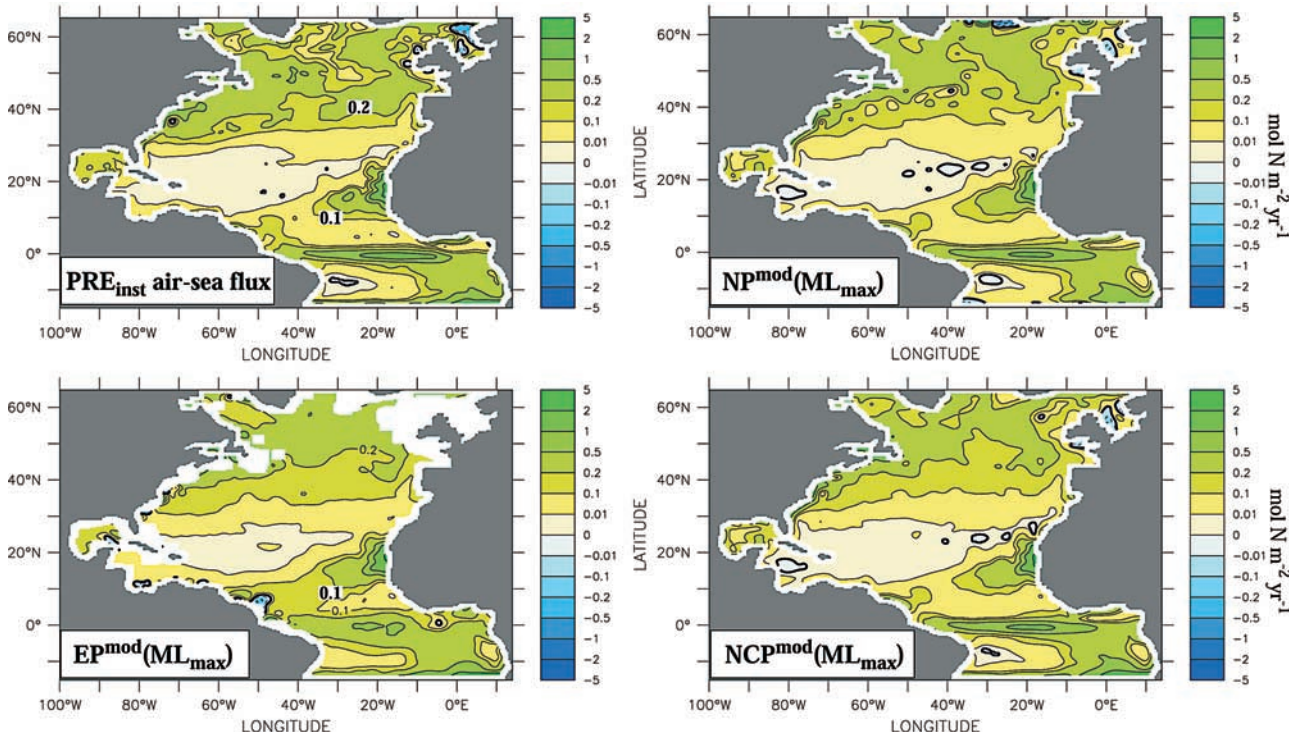

Figure 8. Five-year mean of the air-sea flux of the PRE_{inst} tracer (see text) representing the annual yield of the biological pump, of simulated new production (NP^{mod}_{MLmax}) above the maximum mixed layer depth (ML_{max}), of simulated export production (EP^{mod}_{MLmax}) across ML_{max}, and of simulated net community production (NCP^{mod}_{MLmax}) above ML_{max}. Unit is mol N m^{-2} yr^{-1}.

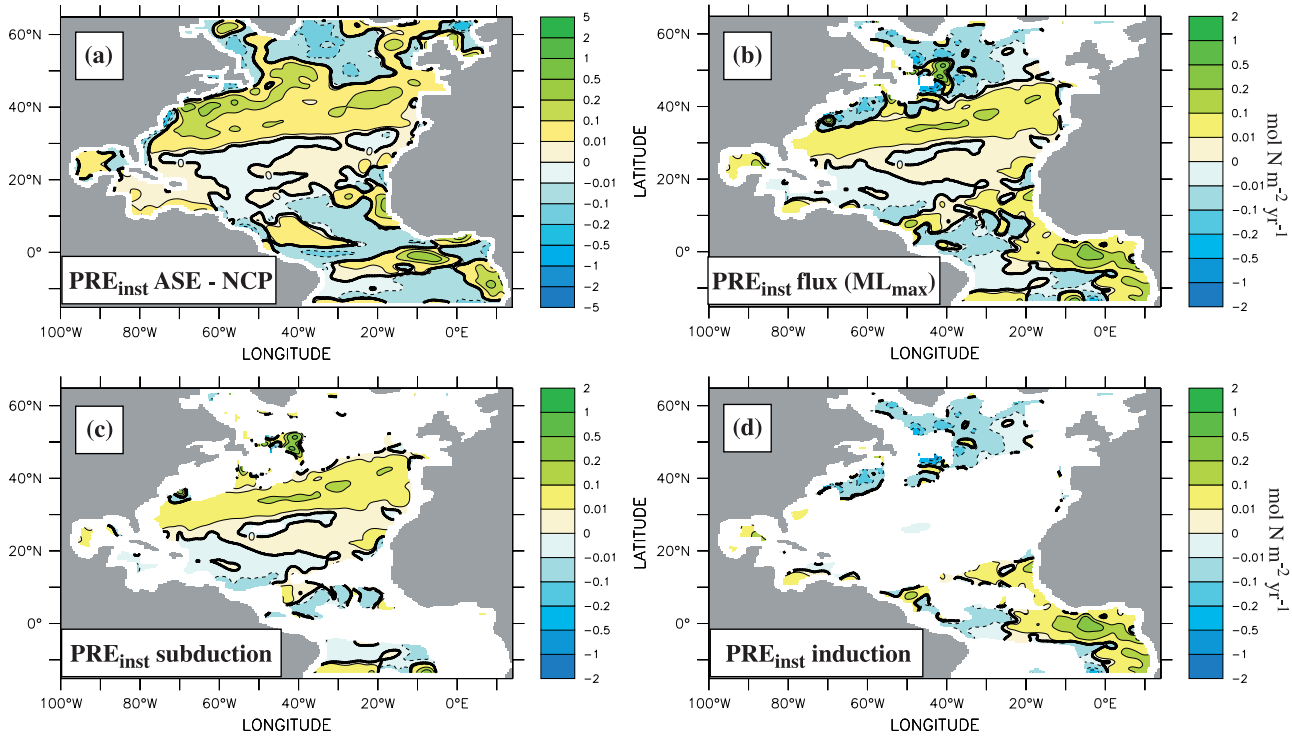

Figure 9. (a) Difference between simulated annual air-sea flux of the PRE_{inst} tracer (see text) and NCP above the maximum mixed layer depth (ML_{max}). (b) Annual transport of the PRE_{inst} tracer across ML_{max}. (c) Annual subduction of PRE_{inst} across ML_{max} in regions with positive subduction rates only. (d) Annual induction of PRE_{inst} across ML_{max} in regions with negative subduction rates only. Figure 9b is the superposition of Figures 9c and 9d. Unit is mol N m^{-2} yr^{-1}, and positive values in all panels indicate export of PRE_{inst} to below ML_{max} thereby increasing biotically effected air-sea fluxes of PRE_{inst} and, by inference, of CO_2.